



HAL
open science

Photophysical properties of porphyrinic covalent cages endowed with different flexible linkers

Daniel Sánchez-Resa, Laëtitia Schoepff, Ryan Djemili, Stephanie Durot, Valérie Heitz, Barbara Ventura

► To cite this version:

Daniel Sánchez-Resa, Laëtitia Schoepff, Ryan Djemili, Stephanie Durot, Valérie Heitz, et al.. Photophysical properties of porphyrinic covalent cages endowed with different flexible linkers. *Journal of Porphyrins and Phthalocyanines*, 2019, 23 (07n08), pp.841-849. <10.1142/S1088424619500925>. <hal-03415521>

HAL Id: hal-03415521

<https://hal.science/hal-03415521v1>

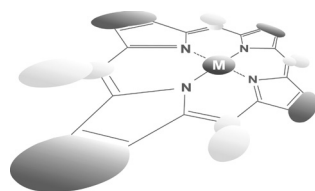
Submitted on 4 Nov 2021

HAL is a multi-disciplinary open access archive for the deposit and dissemination of scientific research documents, whether they are published or not. The documents may come from teaching and research institutions in France or abroad, or from public or private research centers.

L'archive ouverte pluridisciplinaire **HAL**, est destinée au dépôt et à la diffusion de documents scientifiques de niveau recherche, publiés ou non, émanant des établissements d'enseignement et de recherche français ou étrangers, des laboratoires publics ou privés.



HAL Authorization



Photophysical properties of porphyrinic covalent cages endowed with different flexible linkers

Daniel Sánchez-Resa^a, Laetitia Schoepff^b, Ryan Djemili^b, Stéphanie Durot^b,
Valérie Heitz^{*b} and Barbara Ventura^{*a}

^aIstituto ISOF-CNR, Via P. Gobetti 101, 40129 Bologna, Italy

^bLaboratoire de Synthèse des Assemblages Moléculaires Multifonctionnels, Institut de Chimie de Strasbourg, CNRS/UMR 7177, Université de Strasbourg, 4, Rue Blaise Pascal, 67000 Strasbourg, France

This paper is part of the 2019 Women in Porphyrin Science special issue.

Dedicated to Dr. Lucia Flamigni, an excellent scientist and a mentor in the photophysics of porphyrin assemblies.

Received 31 May 2019

Accepted 12 July 2019

ABSTRACT: In-depth photophysical studies of four flexible covalent cages bearing either two free-base porphyrins or one free-base porphyrin and one Zn(II) porphyrin, connected by linkers of different lengths, are reported. In the case of the cages with two free-base porphyrins, exciton coupling between the porphyrins is evidenced by large and split Soret bands in the absorption spectra, but the different length of the linkers has only a slight effect on their emission properties. Strong electronic interactions between the porphyrins are also evidenced for the cages that incorporate a free-base porphyrin and a Zn(II) porphyrin, with a more pronounced splitting of the Soret band for the system with longer linkers. In these cages, following excitation of the Zn-porphyrin component, an almost quantitative energy transfer to the free-base unit occurs, with a rate 1.4 times faster in the cage with longer linkers ($1.4 \times 10^{11} \text{ s}^{-1}$ vs. $1.0 \times 10^{11} \text{ s}^{-1}$). This difference might reflect the more flattened conformation adopted by the cage equipped with longer and more flexible linkers, the latter allowing for a shorter interplanar distance between the porphyrins. The results are discussed in terms of classical and short-range energy transfer mechanisms.

KEYWORDS: porphyrins, molecular cages, photoinduced energy transfer.

INTRODUCTION

The design of functional systems based on molecular capsules has shown great potential in nanochemistry, since these systems can work as nanoreactors, molecular recognition systems or drug carriers, providing a confined environment that enhances molecular reactivity and catalysis [1–3].

Among the different possibilities in the design of molecular cages, the choice of metallated or free-base porphyrins leads to attractive architectures due to their chemical stability and their mimicry of natural

chromophores [1, 4–20]. Indeed, conversion of light energy into chemical energy performed in photosynthesis relies on efficient multistep energy transfer processes between natural chromophores belonging to the family of porphyrin derivatives (chlorophyll or bacteriochlorophyll molecules) organized in antennas that convey the energy towards the reaction center where the first electron transfer step towards a free-base porphyrin derivative occurs [21–27]. The efficiency of such processes is determined by the distance and mutual arrangement of these chromophores, and light-responsive cages have gained interest due to their ability to perform and control energy transfer processes [6, 7, 18, 28].

We have shown that bis-Zn(II) porphyrin cages equipped with four flexible linkers incorporating

*Correspondence to: Valérie Heitz, tel.: 33 (0)3 68 85 13 57, email: v.heitz@unistra.fr, Barbara Ventura, tel.: 0039 051 6399817, email: barbara.ventura@isof.cnr.it.

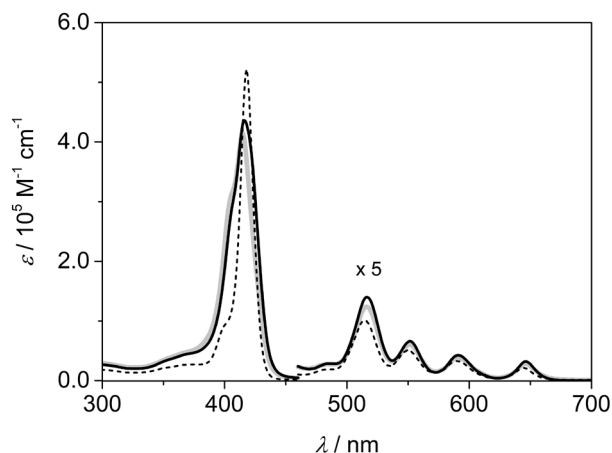


Fig. 1. Absorption spectra of **2H-S-2H** (gray), **2H-L-2H** (black full) and twice the absorption spectrum of **2H-alkyne** (black dashed) in DCM:MeOH (90:10). Absorption in the 460–700 nm region is amplified by a factor of five

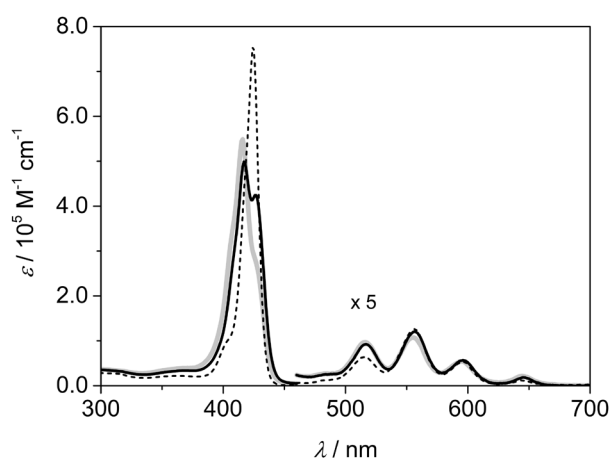


Fig. 2. Absorption spectra of **Zn-S-2H** (gray), **Zn-L-2H** (black full) and the sum of the absorption spectra of **2H-alkyne** and **Zn-alkyne** (black dashed) in DCM:MeOH (90:10). Absorption in the 460–700 nm region is amplified by a factor of five

are in accordance with a more slipped displacement of the porphyrins in **Zn-L-2H** with respect to a cofacial disposition favored in the cage with shorter and more rigid linkers, **Zn-S-2H**, a structural description provided by theoretical modelling performed on our bis Zn-porphyrin cages analogs [32]. As a confirmation, integrated molar absorption coefficients of $1.32 \times 10^9 \text{ M}^{-1} \cdot \text{cm}^{-2}$ and $1.29 \times 10^9 \text{ M}^{-1} \cdot \text{cm}^{-2}$ are calculated for **Zn-S-2H** and **Zn-L-2H**, respectively, values very close to the sum of the coefficients for **2H-alkyne** and **Zn-alkyne** ($1.06 \times 10^9 \text{ M}^{-1} \cdot \text{cm}^{-2}$). To better take into account the coupling interactions, the spectra of the monometallated cages have been compared with the sum of half the spectra of the parent cages containing two identical porphyrins, *i.e.* the bis free-base **2H-S-2H** and **2H-L-2H** studied here and the two dimetallated Zn(II) cages **Zn-S-Zn** and **Zn-L-Zn**

previously reported [32]. The comparison for **Zn-S-2H** and **Zn-L-2H** with the sum of the respective free-base and Zn “half cages” is shown in Fig. S15. It is evident that in both cases the sum overlaps with a good approximation to the experimental spectrum of the monometallated cage, even in the Soret region which is more affected by interporphyrinic exciton coupling. It derives that the cages with two free-base or two Zn-porphyrins can be considered, from the photophysical point of view, as better models for the monometallated cages than the monomeric units **2H-alkyne** and **Zn-alkyne**, due to the strong interactions experienced by the porphyrins within these cages.

Luminescence determinations were performed both at room temperature in DCM:MeOH (90:10) and at 77K in frozen DCM:MeOH (50:50) matrix.

2H-S-2H, **2H-L-2H** and model **2H-alkyne** show similar emission features, with maxima at *ca.* 652 nm and 718 nm, fluorescence quantum yields close to 0.080 and excited state lifetimes on the order of 9.0 ns (Fig. 3 and Table 1), indicating that the emission properties of the free-base porphyrin components are not affected by the conformation of the cages. On the other hand, selective excitation of the free-base unit at 630 nm in **Zn-S-2H** and **Zn-L-2H** (see Fig. S15) results in a lower quantum yield of 0.047 and 0.068, respectively (Table 1), which is paralleled by a reduced lifetime of 6.7 ns and 7.6 ns. This reveals a significant perturbation of the emission properties of the free-base component in the monometallated cages due to the presence of the Zn-porphyrin counterpart. A possible explanation is the close proximity of the Zn center of the metallated porphyrin to the core of the free-base partner, which can lead to a change in molecular symmetry or to an increased intersystem crossing rate [35–37] in the latter.

In order to confirm that the perturbation of the fluorescence features of the free-base porphyrin are due

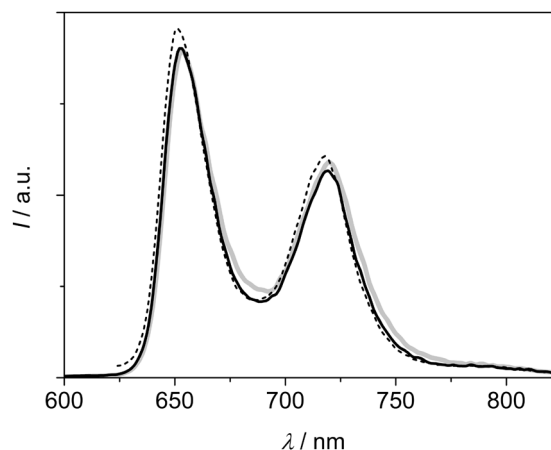


Fig. 3. Corrected emission spectra at room temperature of **2H-S-2H** (gray), **2H-L-2H** (black full) and **2H-alkyne** (black dashed) in DCM:MeOH (90:10). The spectral areas are proportional to the emission quantum yields. $\lambda_{\text{exc}} = 550 \text{ nm}$

Table 1. Luminescence data at room temperature and 77K, in DCM:MeOH (90:10) and (50:50), respectively

		RT			77 K		
		$\lambda_{\max}/\text{nm}^a$	ϕ_f^b	τ/ns^c	$\lambda_{\max}/\text{nm}^a$	τ/ns^c	E/eV
2H-alkyne	$^1\text{H}_2$	652, 718	0.083	8.5	648, 716	11.4	1.91
Zn-alkyne ^f	^1Zn	606, 658	0.040	1.7	599, 656	2.1	2.07
	^3Zn				782	19.2×10^6	1.59
2H-S-2H	$^1\text{2H-2H}$	654, 720	0.078	9.0	648, 716	12.8	1.91
2H-L-2H	$^1\text{2H-2H}$	652, 719	0.082	9.0	647, 715	11.5	1.92
Zn-S-2H	$\text{Zn-}^1\text{2H}$	652, 717	0.047 ^d	6.7	645, 713	11.5	1.92
	$^1\text{Zn-2H}$	606, —	—	0.010 ^e	601, —	—	2.06
	$^3\text{Zn-2H}$				788	15.0×10^6	1.57
Zn-L-2H	$\text{Zn-}^1\text{2H}$	652, 718	0.068 ^d	7.6	644, 712	11.2	1.93
	$^1\text{Zn-2H}$	608, —	—	0.007 ^e	602, —	—	2.06
	$^3\text{Zn-2H}$				787	17.9×10^6	1.58

^aFrom corrected emission spectra. ^bFluorescence quantum yields, measured with reference to TPP (*meso* tetraphenylporphyrin) in aerated toluene as a standard. ^cFluorescence and phosphorescence lifetimes, excitation at 465 nm and 420 nm, respectively. ^dUpon selective excitation of the free-base component at 630 nm. ^eFluorescence lifetimes measured with a streak camera apparatus (time resolution: 1 ps), excitation at 560 nm. ^fFrom Ref. [32].

to the close proximity of the Zn-porphyrin component in the monometallated cages, an equimolar mixture of the models **2H-alkyne** and **Zn-alkyne** has been analyzed. Figure S16 reports absorption and emission spectra of the mixture, compared with the sum of the spectra of the single compounds. The emission spectrum of the mixture is in good agreement with the sum of the spectra of the models (Fig. S16b), indicating that there is no interaction between them in solution.[§] Moreover, a lifetime of 8.6 ns has been measured for the emission of **2H-alkyne** at 720 nm in the mixture, identical to that of the model alone (Table 1).

Upon excitation of both Zn- and free-base porphyrin components in the monometallated cages, the resulting luminescence is dominated by the bands of the free-base unit, while the Zn-porphyrin emission only appears as a weak band at *ca.* 608 nm (Table 1 and Fig. 4). To estimate the extent of the quenching of the Zn-porphyrin component in these cages, the emission of **Zn-S-2H** and **Zn-L-2H** has been compared to that of optically matched solutions of model cages with two free-base units or two Zn-porphyrins, and the results are shown in Fig. 4. The excitation wavelengths were selected according to the

absorption comparison previously described (Fig. S15), aiming at a substantial excitation of the Zn-porphyrin component in the monometallated cages (from 60% to 80% of the absorbed photons). By taking account the portion of excited Zn-porphyrin units in each cage in solution and comparing the intensity of the residual Zn-porphyrin emission at 608 nm with the intensity at the same wavelength for the bis Zn-porphyrin model, it derives that the Zn-porphyrins components are quenched over 90% in **Zn-S-2H** and **Zn-L-2H**. This very efficient quenching can be safely ascribed to an energy transfer process to the free-base porphyrin counterpart. In fact, it is accompanied by a full recovery of the free-base porphyrin emission (Fig. 4): the bands at 652 and 718 nm recover for *ca.* 65% and 80% those of the bis free-base porphyrin model for **2H-S-2H** and **Zn-S-2H**, respectively, mirroring the ratios between the quantum yield of the free-base porphyrin unit in the monometallated cages and that of the same unit in the models (Table 1). A further confirmation of an almost complete Zn→2H energy transfer process comes from the good superimposition of excitation spectra, collected for both **Zn-S-2H** and **Zn-L-2H** at 720 nm where only the free-base porphyrin

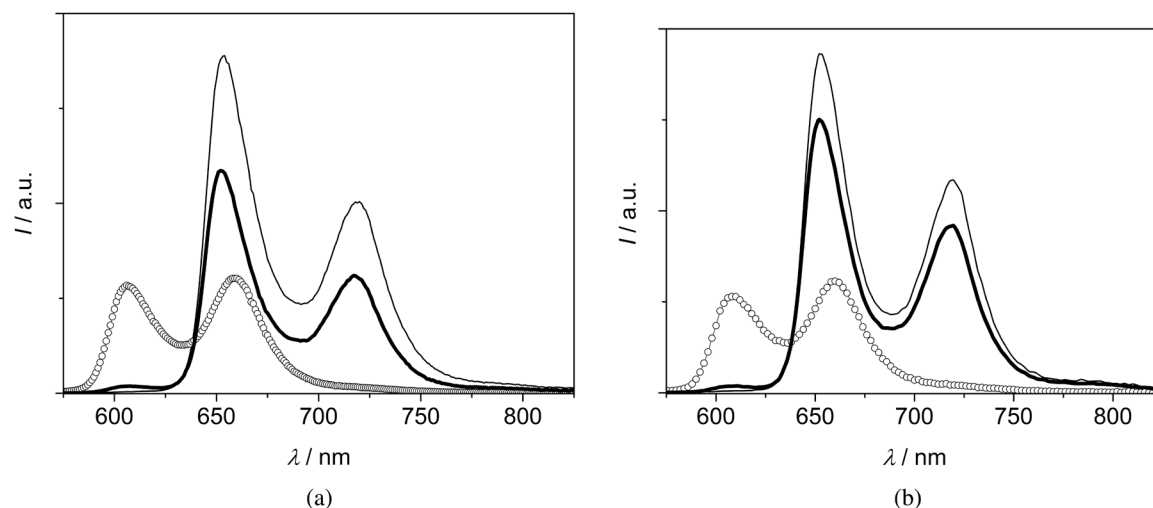


Fig. 4. Corrected emission spectra at room temperature of iso-absorbing solutions of (a) **Zn-S-2H** (black thick) and models **2H-S-2H** (black thin) and **Zn-S-Zn** (dots), excitation at 557 nm (80% of the photons absorbed by the Zn unit in **Zn-S-2H**), $A_{557} = 0.067$; (b) **Zn-L-2H** (black thick) and models **2H-L-2H** (black thin) and **Zn-L-Zn** (dots), excitation at 537 nm (60% of the photons absorbed by the Zn unit in **Zn-L-2H**), $A_{537} = 0.046$; in DCM:MeOH (90:10)

unit emits, and absorption spectra (Fig. S17), indicating that whatever is the excited unit, the energy is conveyed to the lowest singlet excited state of the free-base porphyrin component.

As a verification that the observed energy transfer process is not occurring in freely diffusing porphyrin monomers, an equimolar mixture of models **2H-alkyne** and **Zn-alkyne**, excited at 557 nm, displays an emission spectrum perfectly matching with the sum of the spectra of the models (Fig. S18b), evidencing that there is no quenching of the Zn-porphyrin bands. Moreover, a fluorescence lifetime of 1.7 ns is measured for the mixture at 610 nm, coincident with that of **Zn-alkyne** (Table 1).

Emission measurements at 77K in a DCM:MeOH (50:50) glassy mixture allowed definition of singlet excited state energy levels for all porphyrin components of the four cages and triplet excited state levels for the Zn-porphyrins in the monometallic cages, where phosphorescence was observed in gated mode. Luminescence spectra are shown in Figs S19 and S20 and the relevant data are summarized in Table 1. It can be noticed that, in the monometallated cages, the Zn-porphyrin fluorescence is suppressed similarly to the room temperature case (Fig. S20), indicating that the quenching process occurring within these cages is very efficient even at low temperature.

In order to better characterize the photoinduced events, time-resolved luminescence experiments in the picosecond range were conducted for **Zn-S-2H** and **Zn-L-2H**. The measurements have been performed upon excitation at 560 nm, where the Zn-porphyrin component is prevalently excited, with a 100 fs pulsed laser and acquiring luminescence images with a streak camera apparatus (time resolution: 1 ps). Low laser

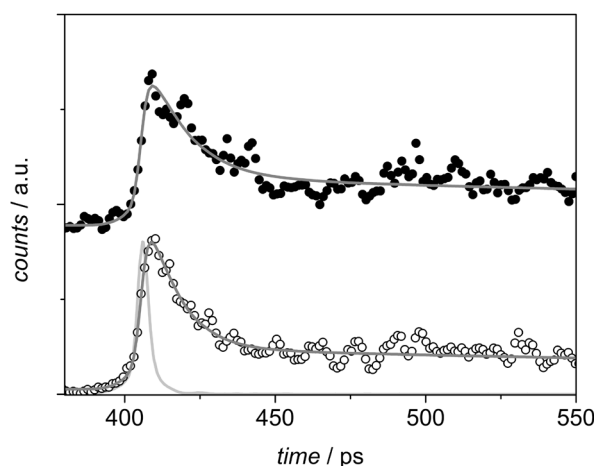


Fig 5. Normalized luminescence decays in the 600–620 nm spectral region for **Zn-S-2H** (full dots) and **Zn-L-2H** (open dots). The bi-exponential fittings are reported as grey lines. The excitation profile is shown in light grey. Excitation at 560 nm (26 $\mu\text{J}/\text{pulse}$)

power and fast image acquisition in analog integration mode were used (see the experimental section for details) to prevent photo-degradation of the compounds. The images identify the existence of a fast process, where a decay in the emission region of the Zn-porphyrin (600–620 nm) is accompanied by a rise in the 700–750 nm spectral region, where only emission from the free-base component is observable (Fig. 5 and Fig. S21). The decay of the Zn-porphyrin luminescence can be fitted with a bi-exponential function where the main component has a lifetime of 10 ps in **Zn-S-2H** and 7 ps in **Zn-L-2H** (Fig. 5). The longer component (accounting for *ca.* 10%

of the decay) can be attributed to a tail of the free-base porphyrin emission or a minor presence of a photo-product. A precise fitting of the rise time of the free-base signal is difficult, but is compatible with the lifetime of the quenched Zn-porphyrin emission (Fig. S21), confirming the sensitization of the free-base singlet excited state upon energy transfer from the Zn-porphyrin component.

The difference between the quenched lifetimes of the Zn-porphyrin component in the two cages is minimal but significant and indicates that the energy transfer process is faster in **Zn-L-2H** than in **Zn-S-2H**. The energy-transfer rate, in fact, is $(1.0 \pm 0.1) \times 10^{11} \text{ s}^{-1}$ and $(1.4 \pm 0.2) \times 10^{11} \text{ s}^{-1}$ for **Zn-S-2H** and **Zn-L-2H**, respectively (see the Experimental section for details). It derives that the process occurs with an efficiency close to 100% in both cages. To better analyze the nature of the energy transfer process, the data have been treated according to the Förster-type mechanism, which is usual between porphyrin chromophores. The overlap integral (J^F) between the emission spectrum of the donor (the bis Zn-porphyrin model) and the absorption spectrum of the acceptor (half the absorption spectrum of the bis free-base porphyrin cage) has been calculated to be $1.96 \times 10^{-14} \text{ cm}^3 \cdot \text{M}^{-1}$ and $1.88 \times 10^{-14} \text{ cm}^3 \cdot \text{M}^{-1}$ for **Zn-S-2H** and **Zn-L-2H**, respectively. An estimation of the geometrical factor K^2 (see the Experimental section) gives values of 0.09 for the cage with short linkers and 1.88 for the cage with long linkers (by considering $\theta_D = \theta_A = 40^\circ \div 90^\circ$ in **Zn-S-2H** and $\theta_D = \theta_A = 15^\circ \div 40^\circ$ in **Zn-L-2H** and ϕ varying from 0° and 60° , according to the geometrical parameters derived for similar cages) [32]. With these parameters, and taking into account the fluorescence quantum yield and the lifetime of the donor in both cases, it is possible to evaluate the donor–acceptor distances that should result in the experimental rate constants on the basis of a Förster-type energy-transfer mechanism. The obtained distances are 6.6 Å and 11.0 Å for **Zn-S-2H** and **Zn-L-2H**, respectively. While the first value is in good agreement with the distance between the two porphyrins estimated in the parent system (7 Å), the second value is not reasonable for a system where the long linkers allow a closer interaction between the porphyrins. Although the estimation of K^2 for these systems involves approximations, in the case of **Zn-L-2H** a possible deviation from the classical Förster treatment can be envisaged, with a weaker short-range dependence of the rate constant, as already observed for closely spaced π systems [38]. At a supposed inter-planar distance of 4 Å estimated for the parent cage [32], we cannot also exclude a contribution from an electron exchange (Dexter) mechanism, that has been found to be operative at very short (<5–6 Å) donor–acceptor distances in cofacial porphyrinic systems [39, 40]. More detailed investigations on the nature of the energy-transfer process are under way.

EXPERIMENTAL

General

All chemicals were of the best commercially available grade and used without further purification. CH_2Cl_2 and CHCl_3 were distilled over CaH_2 before use. Column chromatography was carried out using silica gel (Merck, silica gel 60, 63–200 or 40–63 μm). Mass spectra were obtained by using a Bruker MicroTOF spectrometer in electrospray mode (ES-MS). Nuclear Magnetic Resonance (NMR) spectra for ^1H and ^{13}C were acquired on Bruker AVANCE 300, 400, 500 spectrometers. The ^1H and ^{13}C spectra were referenced to residual solvent peaks. (CDCl_3 , 7.24 and 77.16; CD_2Cl_2 , 5.32 and 53.84; DMSO, 2.50 and 39.52; DMF, 8.03 and 163.15).

Synthesis

Synthesis of monometallated cage Zn-S-2H. Zinc acetate $\text{Zn}(\text{OAc})_2 \cdot 2\text{H}_2\text{O}$ (5.4 mg, 24.8 μmol , 1.1 equiv.) was added to a stirred solution of cage **2H-S-2H** (50.0 mg, 22.5 μmol , 1 equiv.) in 25 mL $\text{CHCl}_3/\text{MeOH}$ (9:1 v/v) at room temperature. Completion was checked by thin layer chromatography (SiO_2 , $\text{CH}_2\text{Cl}_2/\text{CHCl}_3/\text{MeOH}$ 5/5/1). After three hours, the solvent was evaporated and the residue was purified by two consecutive preparative thin layer chromatographies eluted with $\text{CH}_2\text{Cl}_2/\text{CHCl}_3/\text{MeOH}$ 45/45/10 and flash chromatography using $\text{CH}_2\text{Cl}_2/\text{MeOH}$ 95/5) to afford a purple solid (16 mg, 31% yield). ^1H NMR (500 MHz, DMF-d_7): δ (ppm) = 8.49 (8 H, br s, H_{pyr}), 8.42 (8 H, s, H_{pyr}), 8.37 (8 H, s, H_1, H_2), 8.12 (4 H, d, $^3J = 7.6 \text{ Hz}$, $\text{H}_{\text{o'out}}$), 8.08 (4 H, d, $^3J = 7.6 \text{ Hz}$, $\text{H}_{\text{o'out}}$), 7.79 (4 H, d, $^3J = 7.6 \text{ Hz}$, $\text{H}_{\text{m'out}}$), 7.74 (4 H, d, $^3J = 7.6 \text{ Hz}$, $\text{H}_{\text{m'out}}$), 7.14 (4 H, d, $^3J = 7.6 \text{ Hz}$, $\text{H}_{\text{o'in}}$), 7.09 (4 H, d, $^3J = 7.6 \text{ Hz}$, $\text{H}_{\text{o'in}}$), 6.72 (8 H, m, $^3J = 7.6 \text{ Hz}$, $\text{H}_{\text{m'in}}, \text{H}_{\text{m'in}}$), 5.84 (8 H, s, H_1), 5.81 (8 H, s, H_1), 4.70 (16 H, s, H_2, H_2), 3.76 (16H, m, H_3), -3.19 (2 H, s, NH). ^{13}C NMR (126 MHz, DMF-d_7): δ (ppm) = 150.5 (C_2), 146.2 ($\text{C}_{10+10'}$), 143.6 (C_4), 142.0 (C_4'), 137.0 ($\text{C}_{5' \text{out}}$), 136.3 ($\text{C}_{5 \text{out}}$), 135.7–135.4 $\text{C}_7 + \text{C}_7' + \text{C}_{5' \text{in}+5 \text{in}}$, 132.4 (C_1), 127.5 ($\text{C}_{6' \text{out}}$), 127.2 ($\text{C}_{6 \text{out}}$), 126.7 ($\text{C}_{6' \text{in}}$), 126.3 ($\text{C}_{6 \text{in}}$), 125.4 ($\text{C}_{9'}$), 125.3 (C_9), 120.8 (C_3), 120.6 ($\text{C}_{3'}$), 70.6 (C_{12}), 65.3 ($\text{C}_{11'+11}$), 53.9 ($\text{C}_{8'+8}$); pyrrolic ^{13}C $\text{C}_{1'}$ and $\text{C}_{2'}$ are too enlarged to be observed at 298K. ES-MS: m/z (%) calcd for $[\text{C}_{128}\text{H}_{108}\text{N}_{32}\text{O}_8\text{Zn}]^{2+}/2$: 1142.4154; found : 1142.4172 (100) $[\text{M} + 2\text{H}^+]/2$.

Synthesis of monometallated cage Zn-L-2H. Zinc acetate $\text{Zn}(\text{OAc})_2 \cdot 2\text{H}_2\text{O}$ (9.85 mg, 44.9 μmol , 1.1 equiv.) was added to a stirred solution of cage **2H-L-2H** (97.8 mg, 40.8 μmol , 1 equiv.) in $\text{CH}_2\text{Cl}_2/\text{MeOH}$ (9:1 v/v) and refluxed overnight. The solvents were evaporated and the residue was purified by preparative thin layer chromatography eluted with $\text{CH}_2\text{Cl}_2/\text{CHCl}_3/\text{MeOH}$ 44/50/10 to afford a purple solid (26.1 mg, 26% yield). ^1H NMR (500 MHz, DMF-d_7): δ (ppm) = 8.52 (8 H, br

1 s, H_{pyr}), 8.44 (8 H, s, H_{pyr}), 8.29 (4 H, s, H_1), 8.25 (4 H,
 2 s, $H_{1'}$), 8.14 (4 H, d, $^3J = 7.6$ Hz, $H_{\text{o'out}}$), 8.09 (4 H, d,
 3 $^3J = 7.6$ Hz, H_{oout}), 7.71 (4 H, d, $^3J = 7.6$ Hz, $H_{\text{m'out}}$), 7.66
 4 (4 H, d, $^3J = 7.6$ Hz, H_{mout}), 7.22 (4 H, d, $^3J = 7.6$ Hz,
 5 $H_{\text{o'in}}$), 7.17 (4 H, d, $^3J = 7.6$ Hz, $H_{\text{o in}}$), 6.55 (4 H, d, $^3J =$
 6 7.6 Hz, $H_{\text{m'in}}$), 6.52 (4 H, d, $^3J = 7.6$ Hz, $H_{\text{m in}}$), 5.71
 7 (8 H, s, H_1), 5.67 (8 H, s, H_1), 4.66 (8 H, s, $H_{2'}$), 4.65
 8 (8 H, s, H_2), 3.71 (16H, m, H_3), 3.66 (16 H, m, H_4), -2.87
 9 (2 H, s, NH). $^{13}\text{C NMR}$ (126 MHz, DMF- d_7): δ (ppm) =
 10 150.7 (C_2), 146.1 ($C_{10+10'}$), 143.6 (C_4), 142.1 ($C_{4'}$), 136.9
 11 ($C_{5'out}$), 136.2 (C_{5out}), 135.7 ($C_{7'}$), 134.6 ($C_7 + C_{5'in+5 in}$),
 12 132.5 (C_1), 127.5 ($C_{6'out}$), 127.1 (C_{6out}), 126.8 ($C_{6'in}$), 126.3
 13 ($C_6 in$), 125.3 ($C_{6'}$), 125.3 (C_9), 121.1 (C_3), 120.8 ($C_{3'}$),
 14 71.4 (C_{12}), 70.7 (C_{13}), 65.2 ($C_{11'+11}$), 53.8 ($C_{8'+8}$); pyrrolic
 15 $^{13}\text{C } C_{1'}$ and $C_{2'}$ are too enlarged to be observed at 298K.
 16 **ES-MS:** m/z (%) calcd for $[\text{C}_{136}\text{H}_{122}\text{N}_{32}\text{O}_{12}\text{ZnNa}_2]^{2+}/2$:
 17 1252.4498; found : 1252.4521 (100) [$\text{M} + 2\text{Na}^+$]/2;
 18 calcd for $[\text{C}_{136}\text{H}_{122}\text{N}_{32}\text{O}_{12}\text{ZnNa}]^+$: 2481.9104 ; found :
 19 2482.9233 (20).

20 21 Absorption and emission spectroscopy, 22 photophysics

23
24 Spectroscopic grade DCM and MeOH were from Merck
25 and used as received. Silver trifluoromethanesulfonate
26 ($\text{Ag}(\text{OTf})$) was from Sigma–Aldrich and was stored
27 under argon in a sealed vial in dark and dry conditions.
28 $\text{Ag}(\text{OTf})$ solutions were used fresh and kept in the dark
29 during the measurements.

30 Absorption Spectra were recorded with Perkin–Elmer
31 Lambda 650 UV-vis and Perkin–Elmer Lambda 950
32 UV-VIS-NIR spectrophotometers. Integrated absorption
33 coefficients were calculated by plotting molar absorption
34 coefficients as a function of absorption energy (in
35 wavenumbers) and calculating the area under the curves.

36 Emission spectra were collected with an Edinburgh
37 FLS920 fluorimeter, equipped with a Peltier-cooled
38 Hamamatsu R928 PMT (200–850 nm), and corrected
39 for the wavelength-dependent phototube response.
40 Corrected excitation spectra were recorded with the same
41 fluorimeter. Emission quantum yields were evaluated
42 from the area of the luminescence spectra, corrected for
43 the photomultiplier response, with reference to *meso*-
44 tetraphenylporphyrin in aerated toluene ($\phi_{\text{p}} = 0.11$) [41].
45 Measurements at 77K were performed with the same
46 fluorimeter, making use of Pyrex tubes dipped in liquid
47 nitrogen in a quartz Dewar. Gated emission spectra were
48 acquired by using a time-gated spectral scanning mode
49 and a μF920H Xenon flash lamp (pulse width $< 2 \mu\text{s}$,
50 repetition rate between 0.1 and 100 Hz) as excitation
51 source. Spectra were corrected for the wavelength-
52 dependent photomultiplier response. Triplet excited state
53 lifetimes were measured with the same apparatus in the
54 multichannel scaling mode.

55 Fluorescence lifetimes in the nanosecond range were
56 detected by using an IBH Time Correlated Single
57

Photon Counting apparatus with Nano-LED excitation
at 465 nm. Analysis of the decay profiles against time
was performed using the Decay Analysis Software DAS6
provided by the manufacturer.

Fluorescence lifetimes in the ps regime were measured
by means of a Hamamatsu synchroscan streak-camera
apparatus (C10910-05 main unit and M10911-01
synchroscan unit) equipped with an ORCA-Flash 4.0 V2
charge-coupled device (CCD) and an Acton spectrograph
SP2358. As excitation source, a Newport Spectra Physics
Solstice-F-1K-230 V laser system, combined with a
TOPAS Prime (TPR-TOPAS-F) optical parametric
amplifier (pulse width: 100 fs, 1 kHz repetition rate) [42]
was used, tuned at 560 nm. To reduce photo-degradation,
the pump energy on the sample was reduced to 26 μJ /
pulse. Emission from the sample, collected at a right
angle with a 1 mm slit, was focused by means of a
system of lenses into the spectrograph slit. Streak images
were taken in analog integration mode (100 exposures,
exposure time: 2 s). The decays were measured over
emission spectral ranges of 20–40 nm. HPD-TA 9.3
software from Hamamatsu was used for data acquisition
and analysis. The overall time resolution of the system
after deconvolution procedure was 1 ps.

The energy transfer rate in the monometallic cages is
calculated as $k_{\text{en}} = 1/\tau - 1/\tau_0$, in which τ is the lifetime
of the quenched donor unit and τ_0 the lifetime of the
unquenched unit, *i.e.* the lifetime of the reference model
(the Zn-component in the bis Zn-porphyrin cages):
1.7 ns for **Zn-S-Zn** and 1.6 ns for **Zn-L-Zn** [32].
The error for the energy transfer rate value has been
estimated according to the partial derivative methods
and by taking the temporal resolution of the measuring
system as uncertainty on the lifetime value (1 ps for τ ,
measured with the streak camera apparatus, and 0.2 ns
for τ_0 , measured with the Time Correlated Single Photon
Counting equipment). The energy transfer efficiency is
defined as $\eta_{\text{en}} = k_{\text{et}} / (k_{\text{et}} + \tau_0^{-1})$.

The calculation of the energy-transfer rate constant
according to the Förster theory was performed by using
equation (1) [43], where d_{DA} is the distance between the
centers of mass of the donor and acceptor, Φ and τ are the
emission quantum yield and lifetime of the donor, J^{F} the
overlap integral, n the refractive index of the solvent and
 K^2 the orientation factor, calculated according to equation
(2) [44], where θ_{D} and θ_{A} are the angles formed between
the line connecting the donor and acceptor centers
and the transition moments of the donor and acceptor,
respectively, and ϕ is the angle between the projections
of the transition moments on a plane perpendicular to the
line connecting the centers of the donor and the acceptor.

$$k_{\text{en}}^{\text{F}} = \frac{8.8 \times 10^{-25} k^2 \Phi}{n^4 \tau d_{\text{DA}}^6} J^{\text{F}} \quad (1)$$

$$K^2 = (\sin\theta_{\text{D}} \sin\theta_{\text{A}} \cos\phi - 2 \cos\theta_{\text{D}} \cos\theta_{\text{A}})^2 \quad (2)$$

1 Estimated errors are 10% on lifetimes, 20% on
2 quantum yields, 20% on molar absorption coefficients
3 and 3 nm on emission and absorption peaks.

4 CONCLUSION

7 The photophysics of flexible covalent cages bearing
8 either two free-base porphyrins or one free-base porphyrin
9 and one Zn(II) porphyrin, connected by flexible linkers of
10 different lengths, has been investigated in detail by means
11 of steady-state and time-resolved spectroscopic studies.
12 Strong exciton interactions between the porphyrins have
13 been evidenced in all cases, due to the close proximity
14 of these units in the collapsed structure of the cages.
15 The emission features of the porphyrins depend on the
16 composition of the cage and/or on the lengths of the
17 linkers: the free-base units display altered fluorescence
18 quantum yield and lifetime only in the monometallated
19 cages, where the Zn counterpart influences their radiative
20 behavior, with a more important reduction in the cage
21 with shorter linkers. The Zn-porphyrins are quantitatively
22 quenched by a fast energy transfer process that sensitizes
23 the free-base emission in both monometallated cages.
24 This photoinduced process is slightly faster in the cage
25 with longer linkers, probably due to the very short
26 interplanar distance between the porphyrins in this cage,
27 supposed to be around 4 Å. The results highlight the role
28 of the linkers and of the arrangement of the components
29 in the photophysics of flexible porphyrinic cages.

31 Acknowledgments

32 The International Center for Frontier Research in
33 Chemistry, icFRC (www.icfrc.fr), and the LabEx-CSC
34 are gratefully acknowledged for a Ph.D. fellowship
35 to L.S. The Ministry of Education and Research is
36 acknowledged for a Ph.D. fellowship to R.D. We also
37 thank the ANR Agency for the funding of the project
38 ANR 14-CE06-0010 “Switchable cages” and the Italian
39 CNR (Project “PHEEL”). Prof. Isabella Daidone, Dr.
40 Laura Zanetti-Polzi (University of L’Aquila) and Dr.
41 Andrea Barbieri (ISOF-CNR) are thanked for helpful
42 discussion. EC is acknowledged for the NOAH project,
43 grant N. 765297 under H2020-MSCA-ITN-2017.

46 Notes

47 [§] The emission contribution from the model Zn-alkyne
48 in the mixture upon excitation at 630 nm is not negligible
49 at the concentration used, which is optimized for the free-
50 base porphyrin excitation.

52 REFERENCES

- 54 1. Durot S, Taesch J and Heitz V. *Chem. Rev.* 2014;
55 **114**: 8542–8578.
56 2. Chakrabarty R, Mukherjee PS and Stang PJ. *Chem.*
57 *Rev.* 2011; **111**: 6810–6918.

3. Mukhopadhyay RD, Kim Y, Koo J and Kim K. *Acc.*
4 *Chem. Res.* 2018; **51**: 2730–2738. 1
2
4. Balaban TS. *Acc. Chem. Res.* 2005; **38**: 612–623. 3
5. Li W-S, Kim KS, Jiang D-L, Tanaka H, Kawai T,
6 Kwon JH, Kim D and Aida T. *J. Am. Chem. Soc.*
7 2006; **128**: 10527–10532. 4
5
6. Harvey PD, Stern C, Gros CP and Guillard R. *Coord.*
7 *Chem. Rev.* 2007; **251**: 401–428. 7
8
7. Nakamura Y, Aratani N and Osuka A. *Chem. Soc.*
8 *Rev.* 2007; **36**: 831–845. 9
9
8. Satake A and Kobuke Y. *Org. Biomol. Chem.* 2007;
10 **5**: 1679–1691. 11
12
9. Gust D, Moore TA and Moore AL. *Acc. Chem. Res.*
13 2009; **42**: 1890–1898. 14
10. Wasielewski MR. *Acc. Chem. Res.* 2009; **42**:
15 1910–1921. 16
11. Lindsey JS and Bocian DF. *Acc. Chem. Res.* 2011;
17 **44**: 638–650. 18
12. Pellegrin Y and Odobel F. *Coord. Chem. Rev.* 2011;
19 **255**: 2578–2593. 20
21
13. Sprafke JK, Kondratuk DV, Wykes M, Thomp-
22 son AL, Hoffmann M, Drevinskas R, Chen W-H,
23 Yong CK, Kärnbratt J, Bullock JE, Malfois M,
24 Wasielewski MR, Albinsson B, Herz LM, Zigman-
25 tas D, Beljonne D and Anderson HL. *J. Am. Chem.*
26 *Soc.* 2011; **133**: 17262–17273. 26
27
14. Griffith MJ, Sunahara K, Wagner P, Wagner K, Wal-
28 lace GG, Officer DL, Furube A, Katoh R, Mori S and
29 Mozer AJ. *Chem. Commun.* 2012; **48**: 4145–4162. 29
30
15. Wytko JA, Ruppert R, Jeandon C and Weiss J.
31 *Chem. Commun.* 2018; **54**: 1550–1558. 31
32
16. Hong S, Rohman MdR, Jia J, Kim Y, Moon D, Kim
33 Y, Ko YH, Lee E and Kim K. *Angew. Chem.* 2015;
34 **127**: 13439–13442. 34
35
17. Yu C, Long H, Jin Y and Zhang W. *Org. Lett.* 2016;
36 **18**: 2946–2949. 36
37
18. Hwang I-W, Kamada T, Ahn TK, Ko DM, Naka-
38 mura T, Tsuda A, Osuka A and Kim D. *J. Am.*
39 *Chem. Soc.* 2004; **126**: 16187–16198. 39
40
19. Hernández-Eguía LP, Escudero-Adán EC, Pintre
41 IC, Ventura B, Flamigni L and Ballester P. *Chem.* —
42 *Eur. J.* 2011; **17**: 14564–14577. 42
43
20. Durot S, Flamigni L, Taesch J, Dang TT, Heitz V and
44 Ventura B. *Chem. — Eur. J.* 2014; **20**: 9979–9990. 44
45
21. Huber R. *Angew. Chem., Int. Ed. Engl.* 1989; **28**:
46 848–869. 46
47
22. Deisenhofer J and Michel H. *Angew. Chem., Int. Ed.*
48 *Engl.* 1989; **28**: 829–847. 48
49
23. Deisenhofer J, Epp O, Sinning I and Michel H.
50 *J. Mol. Biol.* 1995; **246**: 429–457. 50
51
24. Papiz MZ, Prince SM, Howard T, Cogdell RJ and
52 Isaacs NW. *J. Mol. Biol.* 2003; **326**: 1523–1538. 52
53
25. Roszak AW. *Science* 2003; **302**: 1969–1972. 53
54
26. Umena Y, Kawakami K, Shen J-R and Kamiya N.
55 *Nature* 2011; **473**: 55–60. 55
56
27. Pšenčík J and Tuma R. In *The Structural Basis*
57 *of Biological Energy Generation*, Vol **39**, M.F. 57

- 1 Hohmann-Marriot (ed.) Springer Science+Business
2 Media Dodrecht, 2014; pp 77–109.
- 3 28. Flamigni L, Ventura B, Oliva AI and Ballester P.
4 *Chem. — Eur. J.* 2008; **14**: 4214–4224.
- 5 29. Kocher L, Durot S and Heitz V. *Chem. Commun.*
6 2015; **51**: 13181–13184.
- 7 30. Schoepff L, Kocher L, Durot S and Heitz V. *J. Org.*
8 *Chem.* 2017; **82**: 5845–5851.
- 9 31. Djemili R, Kocher L, Durot S, Peuroren A, Rissanen
10 K and Heitz V. *Chem. — Eur. J.* 2018; **25**: 1 – 8.
- 11 32. Zanetti-Polzi L, Amadei A, Djemili R, Durot S,
12 Schoepff L, Heitz V, Ventura B and Daidone I. *J.*
13 *Phys. Chem. C* 2019; **123**: 13094–13103.
- 14 33. Ishihara S, Labuta J, Van Rossom W, Ishikawa D,
15 Minami K, Hill JP and Ariga K. *Phys. Chem. Chem.*
16 *Phys.* 2014; **16**: 9713–9746.
- 17 34. Ding Y, Zhu W-H and Xie Y. *Chem. Rev.* 2017; **117**:
18 2203–2256.
- 19 35. Fransson T, Saue T and Norman P. *J. Chem. Theory*
20 *Comput.* 2016; **12**: 2324–2334.
- 21 36. Minaev B and Ågren H. *Chem. Phys.* 2005; **315**:
22 215–239.
- 23
24
25
26
27
28
29
30
31
32
33
34
35
36
37
38
39
40
41
42
43
44
45
46
47
48
49
50
51
52
53
54
55
56
57
37. Horiuchi H, Terashima K, Sakai A, Suda D, Yoshi-
hara T, Kobayashi A, Tobita S and Okutsu T. *J. Pho-*
3 *tochem. Photobiol. Chem.* 2016; **321**: 72–78.
- 4 38. Wong KF, Bagchi B and Rossky PJ. *J. Phys. Chem.*
5 *A* 2004; **108**: 5752–5763.
- 6 39. Faure S, Stern C, Guillard R and Harvey PD. *J. Am.*
7 *Chem. Soc.* 2004; **126**: 1253–1261.
- 8 40. Cho HS, Jeong DH, Yoon M-C, Kim YH, Kim
9 Y-R, Kim D, Jeoung SC, Kim SK, Aratani N, Shin-
10 mori H and Osuka A. *J. Phys. Chem. A* 2001; **105**:
11 4200–4210.
- 12 41. Seybold PG and Gouterman M. *J. Mol. Spectrosc.*
13 1969; **31**: 1–13.
- 14 42. Briš A, Trošelj P, Margetić D, Flamigni L and Ven-
15 tura B. *ChemPlusChem* 2016; **81**: 985–994.
- 16 43. Förster Th. *Discuss. Faraday Soc.* 1959; **27**: 7–17.
- 17 44. Van Der Meer BW, Coker III G and Simon S-Y
18 Chen. In *Resonance Energy Transfer: Theory and*
19 *Data*, Wiley VCH Weinheim, 1994; pp. 55–83.
- 20
21
22
23
24
25
26
27
28
29
30
31
32
33
34
35
36
37
38
39
40
41
42
43
44
45
46
47
48
49
50
51
52
53
54
55
56
57